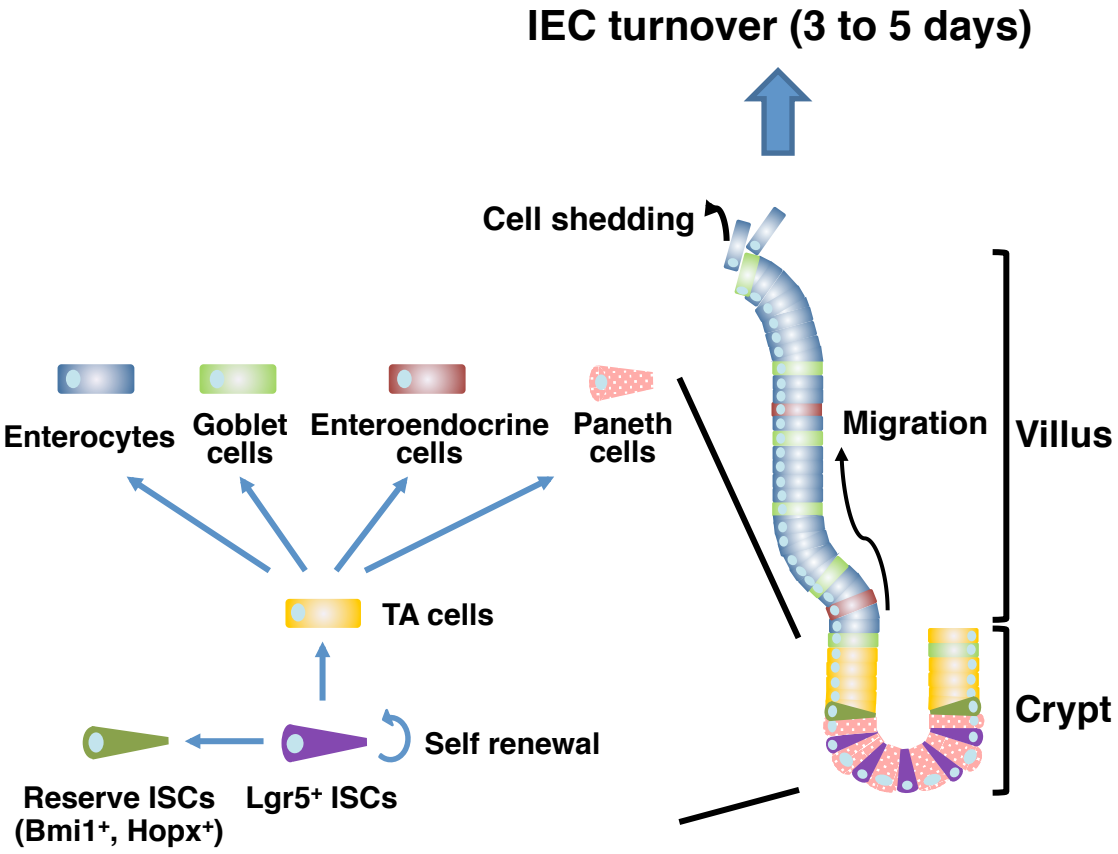

FIG S1 IEC turnover and intestinal homeostasis. Lgr5$^+$ intestinal stem cells (ISCs), which reside in a region near the base of intestinal crypts, engage in self-renewal and generate transient amplifying (TA) cells as well as reserve ISCs. TA cells divide rapidly and differentiate into the various cell lineages of mature intestinal villi, including enterocytes, goblet cells, enteroendocrine cells, and Paneth cells. Cells of the first three of these four lineages mature and migrate up the crypt toward the tip of intestinal villi, whereas Paneth cells travel down to the crypt bottom. The mature cells die and are shed into the intestinal lumen. The turnover of IECs—in particular, that of absorptive enterocytes—is 3 to 5 days in mouse and is strictly regulated to maintain intestinal epithelial homeostasis.

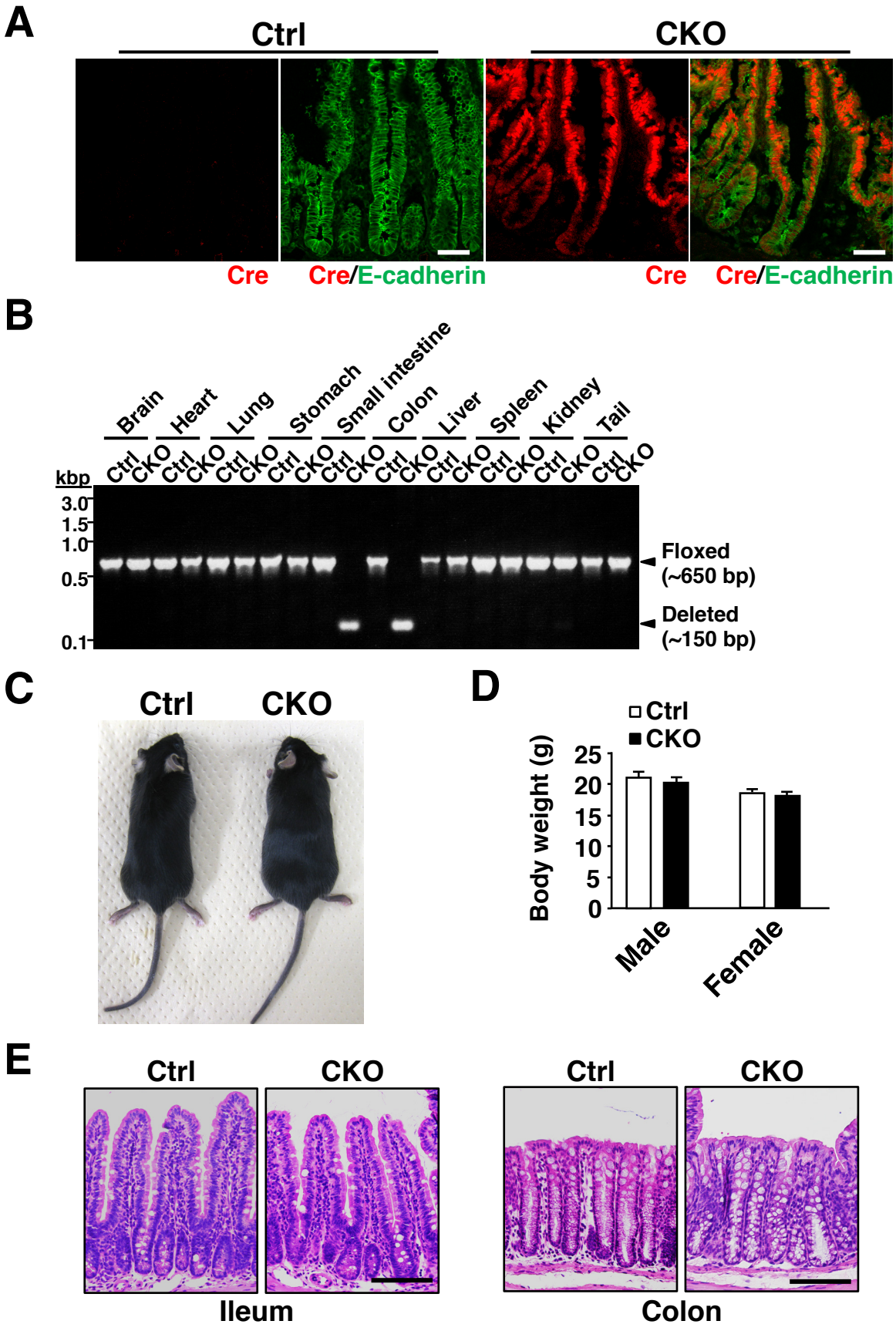

FIG S2 Similarity in gross appearance and intestinal epithelial morphology between control and Csk CKO mice at 8 weeks of age. (**A**) Frozen sections of the ileum from 8-week-old control or Csk CKO mice were subjected to immunostaining with antibodies to Cre (red) and E-cadherin (green). The expression of Cre was observed in gut cells, such as the stem cells and IECs, at the crypt-villus axis. Scale bars, 50 μm. (**B**) Genomic DNA extracted from the indicated organs of adult control (Ctrl) or Csk CKO mice was subjected to PCR analysis with primers specific for deleted or floxed alleles of *Csk*. Data are representative of three separate experiments. (**C**) Representative control and Csk CKO male mice. (**D**) Body weight of control (male, $n = 5$; female, $n = 6$) and Csk CKO (male or female, $n = 7$) mice. Data are means ± SEM. (**E**) Hematoxylin-eosin staining of paraffin-embedded sections of the ileum and colon from control or Csk CKO mice. Scale bars, 100 μm.

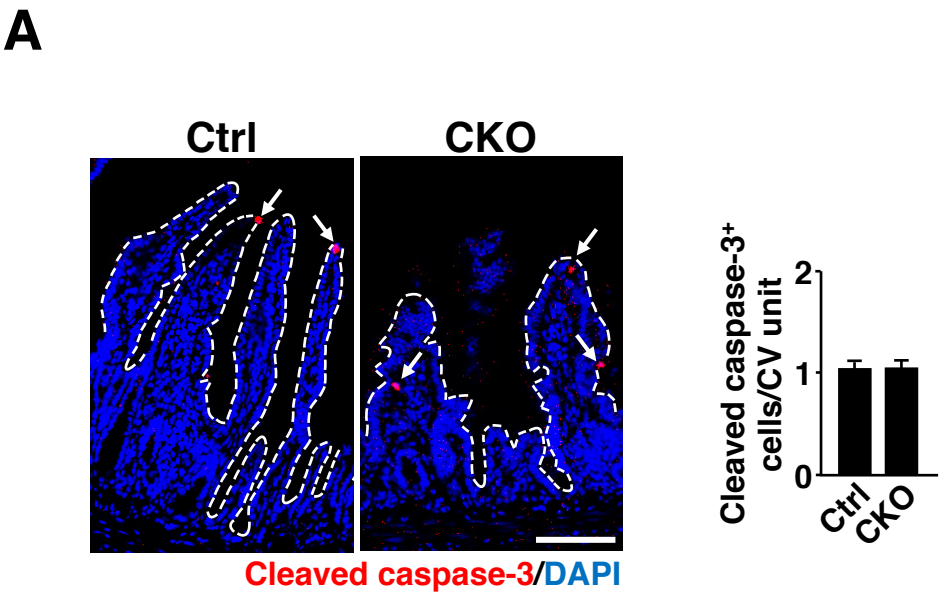

FIG S3 Lack of effect of Csk ablation on IEC apoptosis and the enteroendocrine cell population. (**A**) Frozen sections of the ileum from 8-week-old control or Csk CKO mice were subjected to immunostaining with antibodies to cleaved caspase-3 (red) and to staining of nuclei with DAPI (blue) (left panel). Arrows indicate cells positive for cleaved caspase-3. Dashed lines indicate the boundary of villi. Scale bar, 100 μm. The number of cells positive for cleaved caspase-3 per crypt-villus (CV) unit in such sections was also determined (right panel). (**B**) Frozen sections of the ileum from 8-week-old control or Csk CKO mice were subjected to immunostaining with antibodies to chromogranin A (CgA, red) and to staining of nuclei with DAPI (blue) (left panel). Arrows indicate chromogranin A–positive (CgA^+) cells. Scale bar, 100 μm. Dashed lines indicate the boundary of villi. The number of chromogranin A–positive enteroendocrine cells per villus in such sections was also determined (right panel). Quantitative data (**A** and **B**) are means ± SEM for 90 villi from a total of three mice per genotype.

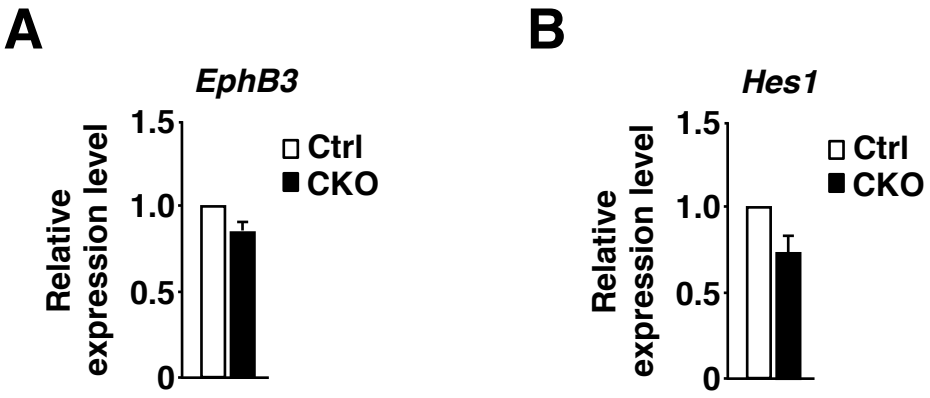

FIG S4 Effect of Csk ablation on *EphB3* or *Hes1* expression in crypts. (A and **B)** The abundance of *EphB3* (**A**) or *Hes1* (**B**) mRNA in crypts isolated from the small intestine of 8-week-old control or Csk CKO mice was determined by quantitative RT-PCR analysis. The amount of *EphB3* or *Hes1* mRNA was normalized by that of *Gapdh* mRNA and then expressed relative to the normalized value for control mice. Data are means ± SEM (n = 5 for EphB3, n = 3 for Hes1).

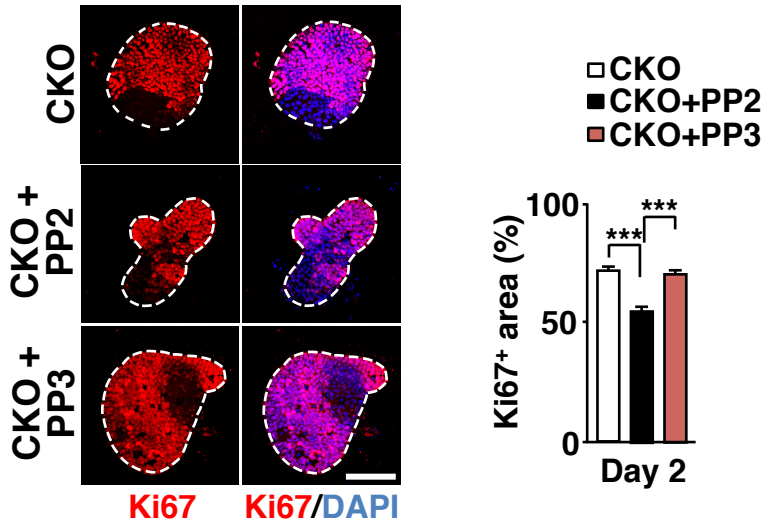

FIG S5 Effect of the SFK inhibitor PP2 on the proliferative phenotype of Csk-deficient intestinal organoids. Intestinal organoids from the jejunum of 8-week-old Csk CKO mice were cultured in the presence of PP2 (10 μM), PP3 (10 μM), or vehicle (DMSO) for 2 days and then subjected to immunostaining with antibodies to Ki67 (red) and to staining of nuclei with DAPI (blue) (left panel). Dashed lines indicate the boundary of intestinal organoids. Scale bar, 100 μm. The Ki67-positive area was also determined as a percentage of the total organoid area (right panel). Quantitative data are means ± SEM for a total of 75 organoids per group in three separate experiments. $^{***}P < 0.001$ (ANOVA and Turkey's test).

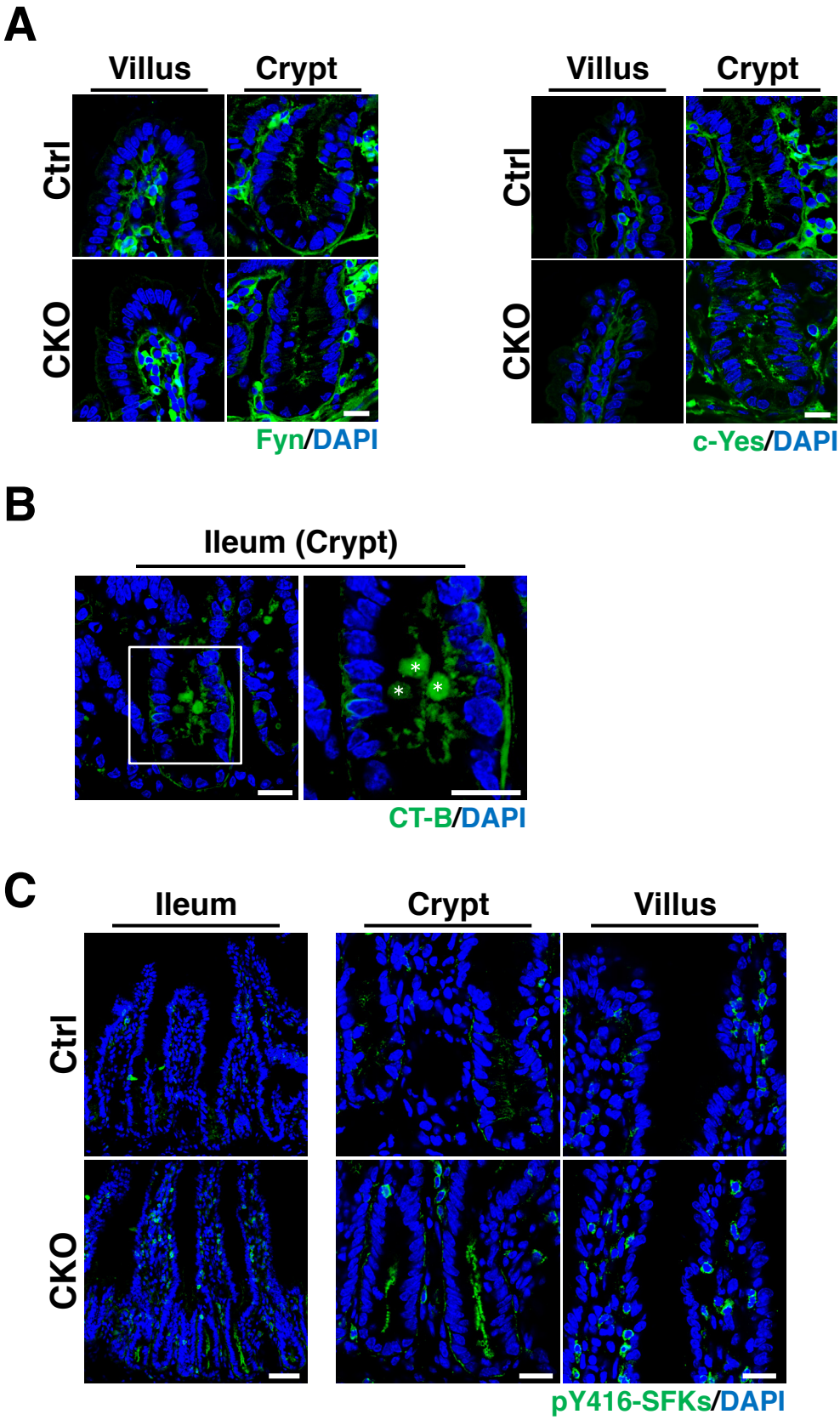

FIG S6 Localization of Fyn, c-Yes, and the ganglioside GM1, as well as autophosphorylation of SFKs, at the apical side of IECs. (**A**) Frozen sections of the ileum from control or Csk CKO mice at 8 weeks of age were subjected to immunostaining with antibodies to Fyn (green) or to c-Yes (green). Nuclei were stained with DAPI (blue). Scale bars, 20 μm. (**B**) Frozen sections of the ileum from control or Csk CKO mice at 8 weeks of age were stained with Alex Fluor 488–conjugated cholera toxin B subunit (CT-B, green) and with DAPI (blue). The boxed region in the left image is shown at higher magnification in the right image. Asterisks indicate nonspecific staining of goblet cell mucin. Scale bars, 20 μm. (**C**) Frozen sections of the ileum from control or Csk CKO mice at 8 weeks of age were subjected to immunostaining with antibodies to autophosphorylated SFKs (pY416-SFKs, green) and staining with DAPI (blue). Scale bars, 50 μm (left images), 20 μm (middle and right images).

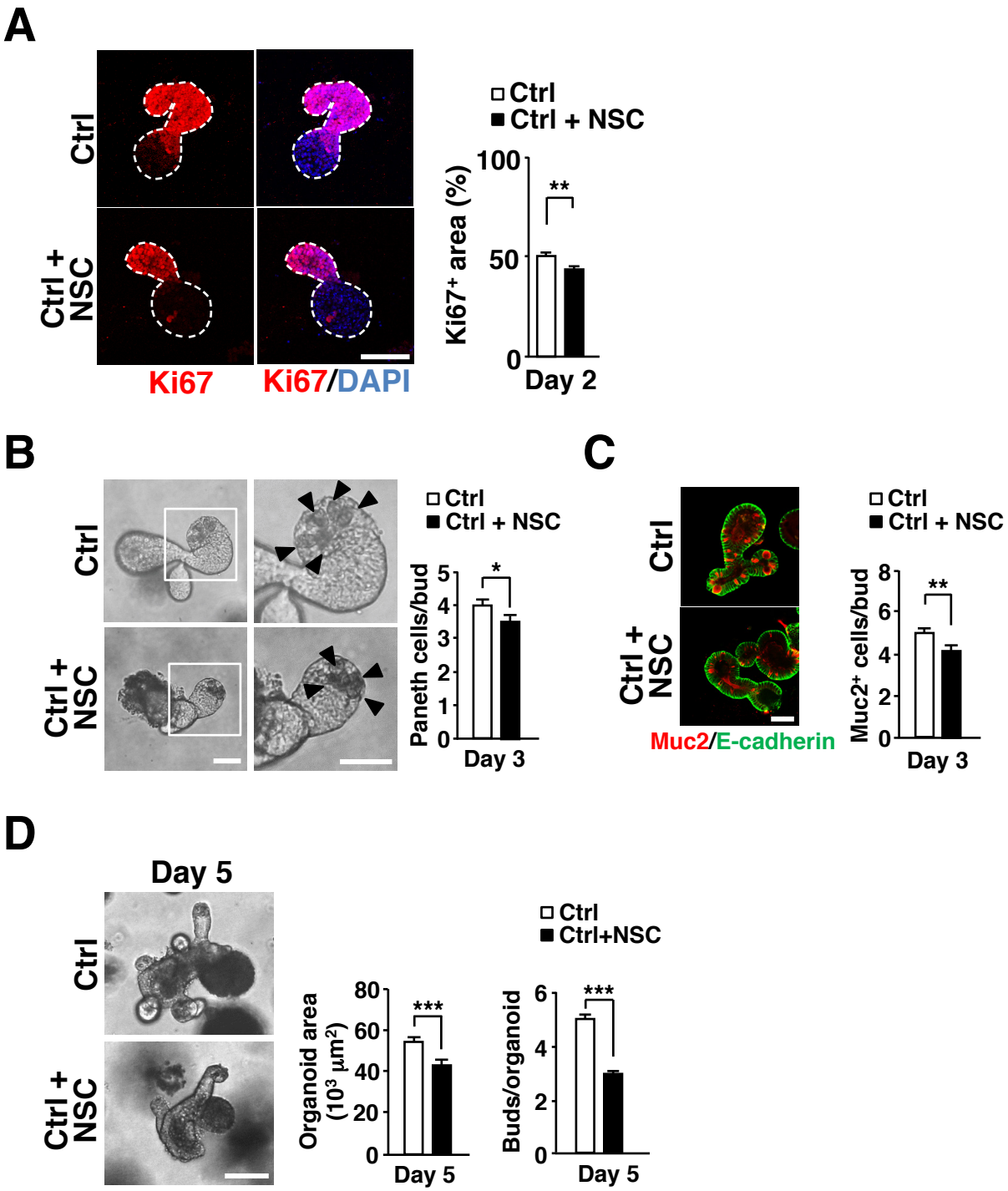

FIG S7 Effect of a Rac inhibitor on the development of intestinal organoids. (**A**) Intestinal organoids derived from the jejunum of 8-week-old control mice were cultured in the absence or presence of the Rac inhibitor NSC23766 (NSC, 50 µM) for 2 days and then subjected to immunostaining with antibodies to Ki67 (red) and to staining of nuclei with DAPI (blue) (left panel). Dashed lines indicate the boundary of intestinal organoids. Scale bar, 100 µm. The Ki67-positive area was also determined as a percentage of the total organoid area in such images (right panel). (**B**) Intestinal organoids cultured for 3 days as in (**A**) were examined by light microscopy (left panel). Boxed regions in the left images are shown at higher magnification in the right images. Arrowheads indicate granule-containing Paneth cells. Scale bars, 50 µm. The number of granule-containing Paneth cells per bud was also determined in such images (right panel). (**C**) Intestinal organoids cultured for 3 days as in (**A**) were subjected to immunostaining with antibodies to Mucin 2 (red) and to E-cadherin (green) (left panel). Scale bar, 50 µm. The number of Mucin 2–positive cells per bud was also determined in such images (right panel). (**D**) Intestinal organoids cultured for 5 days as in (**A**) were examined by light microscopy (left panel). Scale bar, 100 µm. Organoid area (middle panel) and the number of buds per organoid (right panel) were also determined in such images. Quantitative data are means ± SEM for a total of 75 organoids [(**A**) and middle panel of (**D**)], 60 buds (**B**), 45 buds (**C**), or 60 organoids [right panel of (**D**)] per group in three separate experiments. $^{*}P < 0.05$, $^{**}P < 0.01$, $^{***}P < 0.001$ (Student's *t* test).

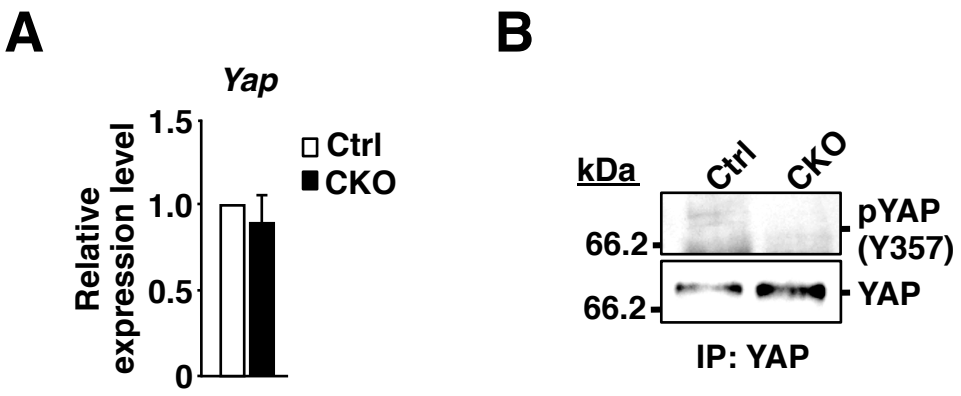

FIG S8 Lack of effect of Csk ablation on *Yap* expression and tyrosine phosphorylation of YAP in crypts of the small intestine. (**A**) Crypts from the small intestine of 8 week-old control or Csk CKO mice were subjected to quantitative RT-PCR analysis of *Yap* mRNA, the amount of which was normalized by that of *Gapdh* mRNA and then expressed relative to the normalized value for control mice. Data are means ± SEM ($n = 5$). (**B**) Lysates of crypts isolated from the small intestine of 8 week-old control or Csk CKO mice were subjected to immunoprecipitation (IP) with antibodies to YAP, and the resulting precipitates were subjected to immunoblot analysis with the same antibodies and with antibodies to Tyr^{357}-phosphorylated YAP. Data are representative of three separate experiments.